Supplement of Earth Surf. Dynam., 14, 247–268, 2026
https://doi.org/10.5194/esurf-14-247-2026-supplement

Earth Surface Dynamics
Open Access
EGU

Supplement of

Limited influence of bedrock strength on river profiles: the dominant role of sediment dynamics

Nanako Yamanishi and Hajime Naruse

Correspondence to: Nanako Yamanishi (yamanishi.nanako.23r@gmail.com)

S1: Sensitivity in the variables of SFDM, ASPM, and SPACEM

We conducted a sensitivity analysis on the parameters for which literature values were used. We used literature values for nondimensional critical shear stress $\tau_c^\star$, friction coefficient C_f, erosional efficiency β_0, and bedload ratio a in SFDM calculation, slope exponent n and drainage area exponent m in ASPM, slope exponent n,drainage area exponent m, and sediment erodibility K_{sed}. For each parameter, its value was varied within the allowable range, and the optimization was repeated to minimize the root mean square (RMS) error between the modeled and observed topography using the modified coefficient. This sensitivity analysis was conducted only for the Gohyaku River; therefore, the RMS is defined using the following equation:

$$RMS = \sqrt{\frac{1}{N}\sum_{i=1}^{n}\left(z^{O}_{n,\mathrm{gohyaku}} - z^{C}_{n,\mathrm{gohyaku}}\right)^2}$$

where $z^{O}_{n,\mathrm{gohyaku}}$ and $z^{C}_{n,\mathrm{gohyaku}}$ represent the observed and calculated elevation of Gohyaku River, respectively. The optimal parameters were determined by the Bayesian optimization method using the python package Optuna (Akiba et al., 2019).

The result of the sensitivity analysis indicated that, in the SFDM, variations in any of the parameters result in only minor changes in the calculated river profiles (Figs., S1–S8). For the nondimensional critical shear stress $\tau_c^\star$ and friction coefficient C_f, changes in RMS were extremely small, remaining within 0.01 (Figs. S1‑S4). In contrast, variations in the erosional efficiency β_0 around 1.0 x 10^{-5} produced minor gradient changes associated with lithological effects in the calculated profiles (Figs. S5‑S6). The parameter β in Eq. (8) ranges from 1.9×10^{-5} to 1.7×10^{-4} (Inoue et al., 2017). The RMS remained stable at around a value of 0.0001 adopted in this study. For the bedload ratio a, the optimized coefficient exhibited oscillatory behavior as a increases; however, the results were relatively stable around a = 0.14 (Takayama, 1965), which is the value used in the present calculations (Figs. S7‑S8).

In the ASPM, variations in both parameters lead to substantial changes in the calculated river profile (Figs., S9‑S12). When the slope exponent n ranges from 0.2 to 1.4, channel gradients associated with lithological contrasts became slightly smoother, and no large changes in gradient were observed (Figs. S9‑S10). In contrast, when n values exceeded around 1.5, the calculated river profiles deviated markedly from the observed topography. Previous studies have reported n falls within the range 0‑2 (Whipple and Tucker, 1999). The value adopted in this study (n = 1.0) lies within the range in which channel gradients remain relatively stable.

When the drainage area exponent m exceeded 0.5, the calculated river profiles generally agreed well with the observed topography and exhibited only minor changes in channel gradient (Figs. S11‑S12). Conversely, for m values of 0.4 or lower, the calculated

profiles increasingly deviated from the observed topography. Values of m below 0.3 were excluded from the analysis because the calculations failed to converge stably; in these cases, modeled elevations became extremely steep, exceeding 1000 m. Based on these results, the value of m = 0.5 adopted in this study lied within a relatively stable range.

In the SPACEM, channel gradients were less sensitive to variations in the slope exponent n than in the ASPM (Figs. S13‑S14). Values of n below 0.7 were excluded from the analysis because the calculations did not converge stably. For values of 0.7 and higher, however, the results were generally stable. Accordingly, the value of m = 0.75 adopted in this study lied within a stable range (Figs. S15‑S16). Previous studies have reported that K_{sed} generally falls within the range 10^{-6}–10^{-4} (Guryan et al., 2024). Consistent with this, variations in K_{sed} produced only minor changes in channel gradients, and the RMS values exhibit little variation (Figs. S17‑S18).

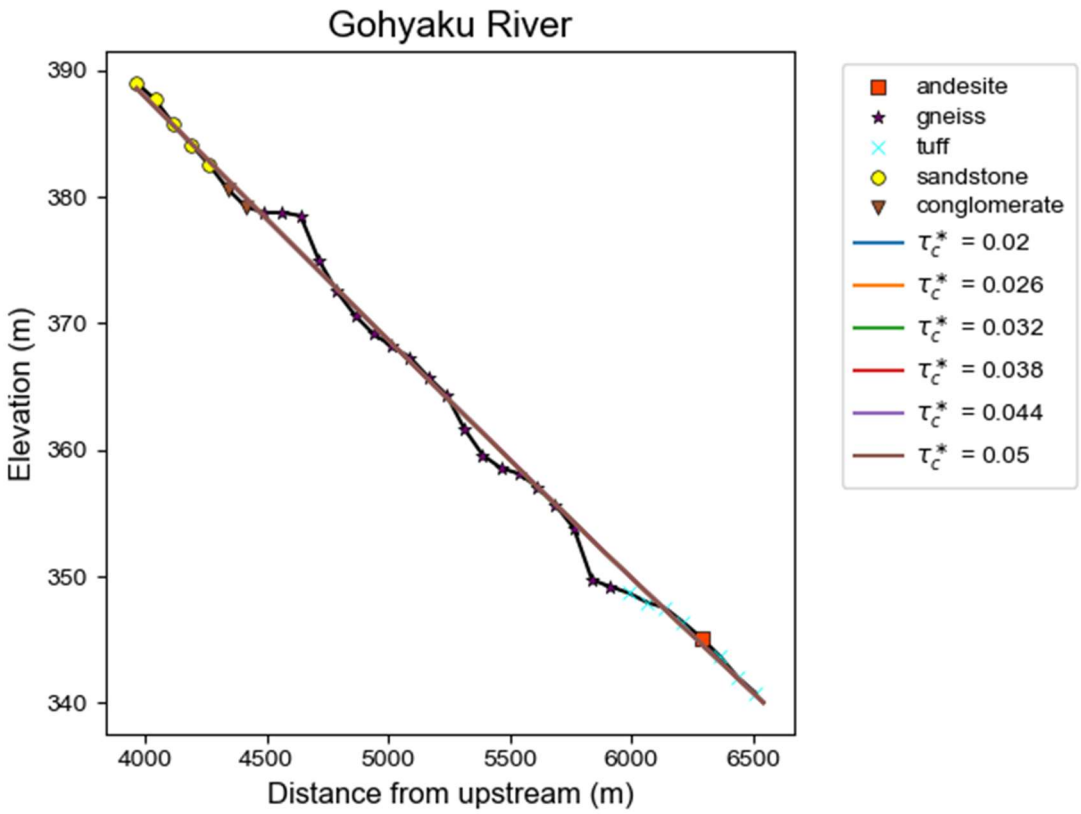

Figure S1. SFDM results of the Gohyaku River obtained by varying the value of the critical Shields stress τ_c^*. Color dots indicate lithology along Gohyaku River (same as Fig.4), and the colored line represents the optimized model result. Within the tested range, changes in the critical Shields number do not significantly affect the optimized results.

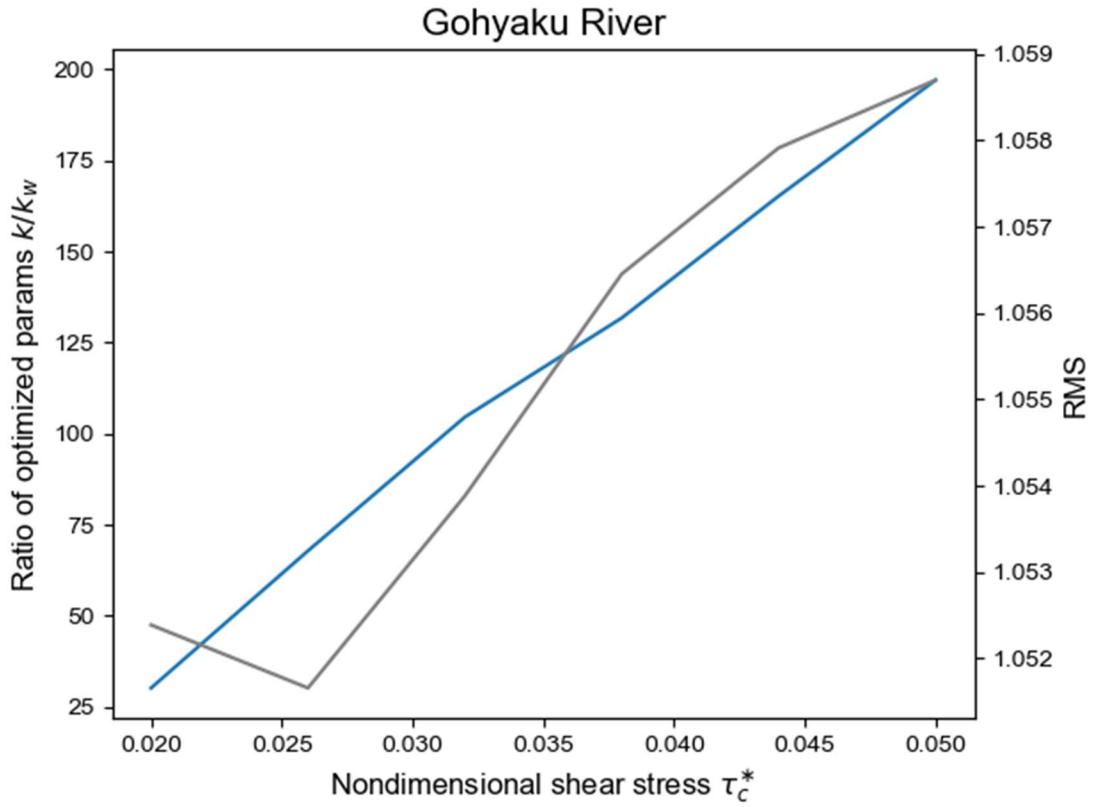

Figure S2. Relationship between nondimensional critical shear stress and ratio of optimized params and RMS. X-axis shows the log scale of nondimensional critical shear stress τ_c^*, and y-axis shows the ratio of optimized params k/k_w. The blue line represents the change of optimized params depending on the nondimensional critical shear stress τ_c^*. The grey line represents the change of RMS. The ratio of optimized params k/k_w is approximately proportional to nondimensional critical shear stress.

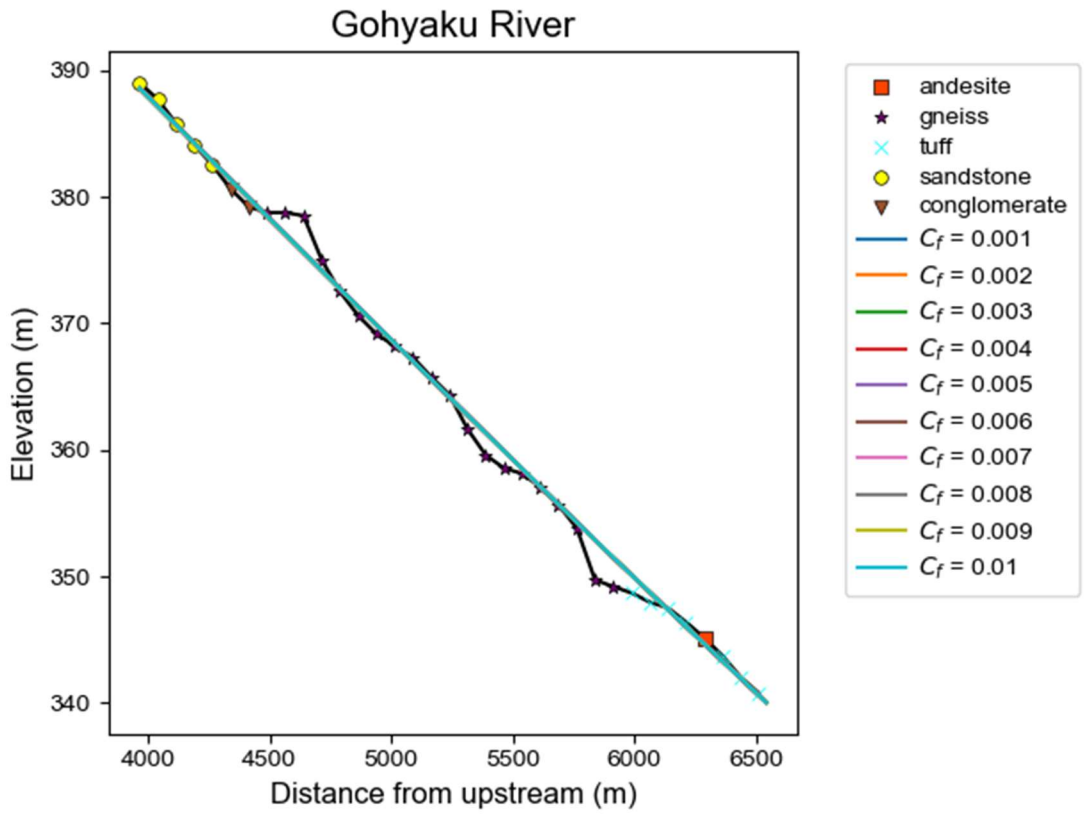

Figure S3. SFDM results of the Gohyaku River obtained by varying the value of friction coefficient C_f. Color dots indicate lithology along Gohyaku River (same as Fig.4), and the colored line represents the optimized model result. Within the tested range, changes in the friction coefficient do not significantly affect the optimized results.

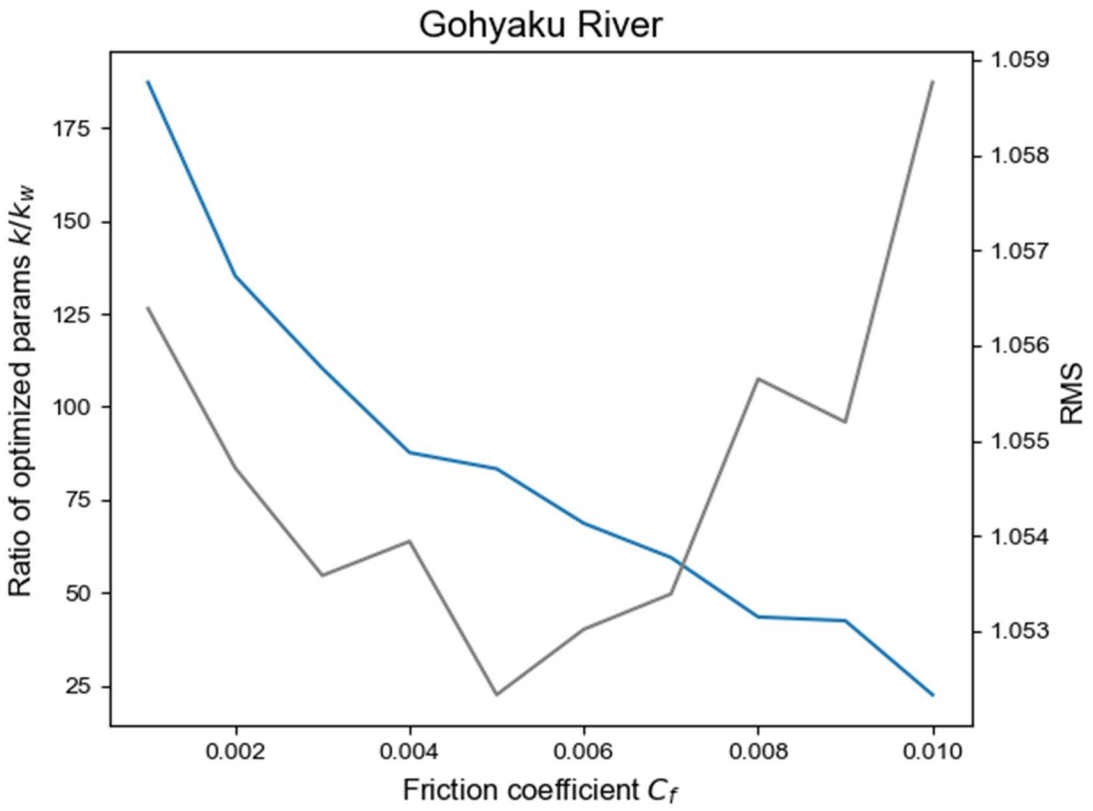

Figure S4. Relationship between friction coefficient and ratio of optimized parameters and RMS. X-axis shows the value of friction coefficient C_f, and the left Y-axis indicates the ratio of optimized parameters k/k_w, while the right Y-axis shows RMS. Blue line represents changes in the optimized parameter ratios depending on the friction coefficient C_f. Grey line represents the change of RMS. The ratio of optimized params k/k_w is approximately inversely proportional to friction coefficient C_f.

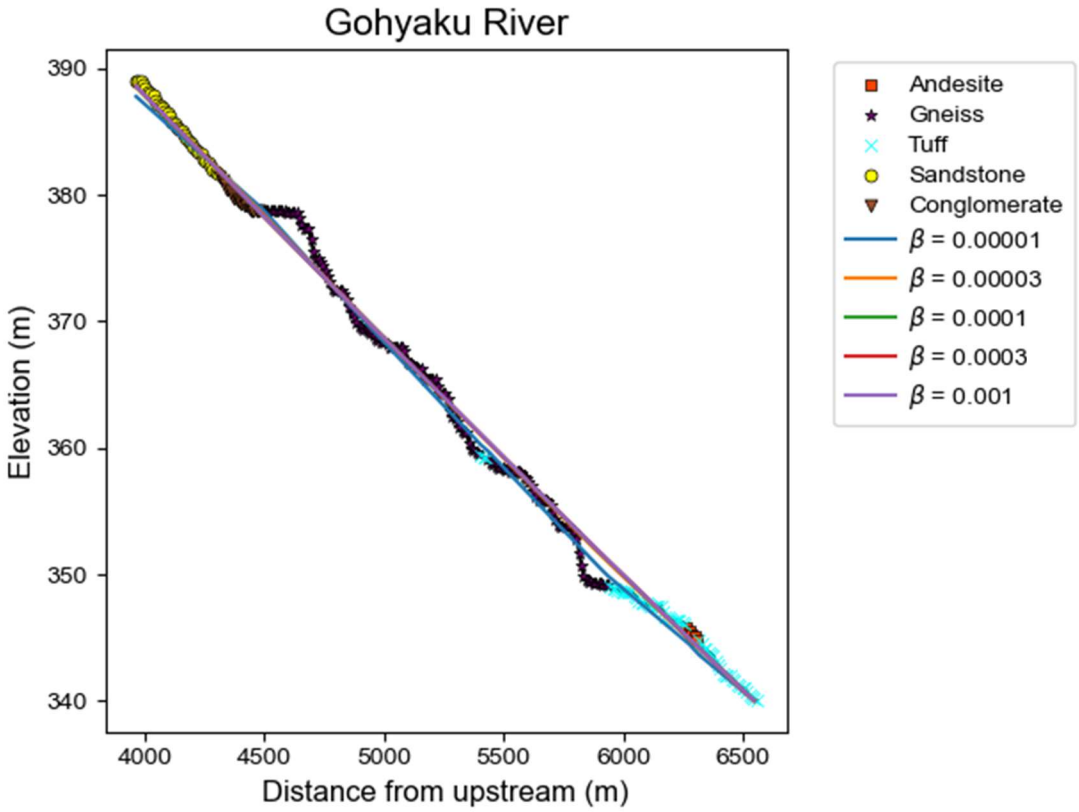

Figure S5. SFDM results of the Gohyaku River obtained by varying the erosional efficiency parameter β_0. Color dots indicate lithology along Gohyaku River (same as Fig.4), and the colored line represents the optimized model result. When β_0 is equal to 0.00001, the modeled river profile exhibits a slight lithological influence.

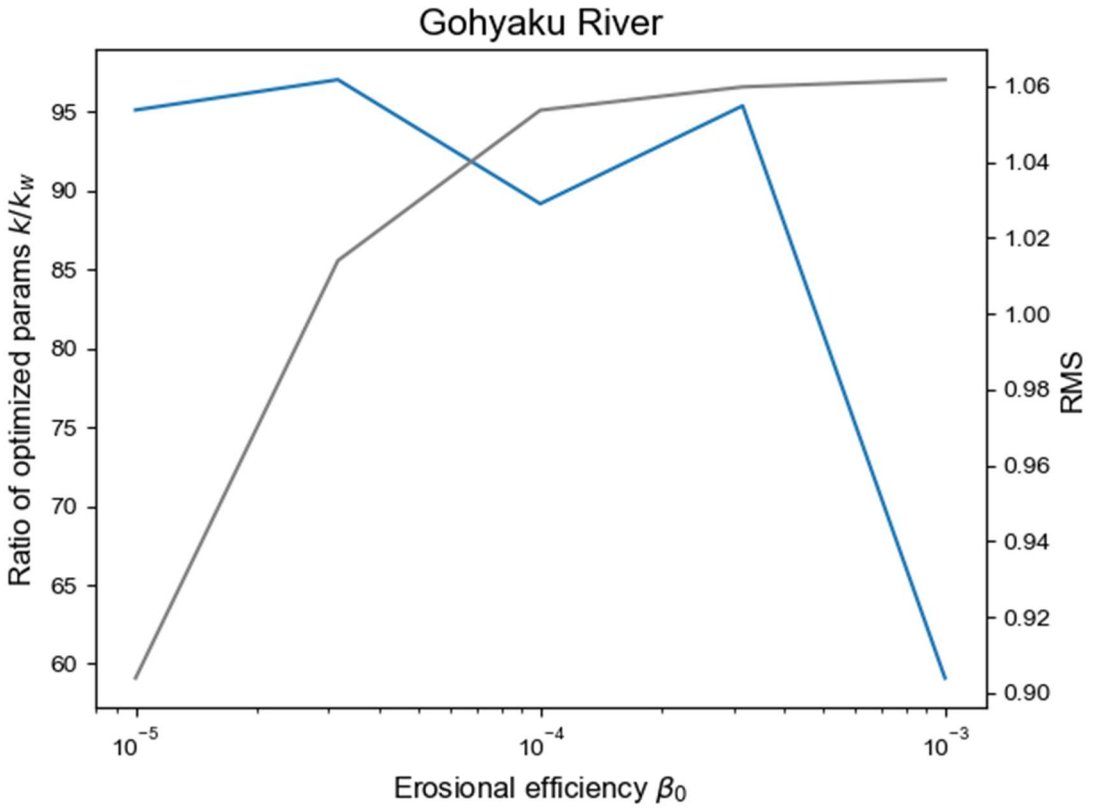

Figure S6. Relationship between erosional efficiency β_0. ratios of optimized parameters, and RMS. X-axis shows the logarithmic scale of erosional efficiency β_0, and the left Y-axis indicates the ratio of optimized parameters k/k_w, while the right Y-axis shows RMS. Blue line represents changes in the optimized parameter ratios depending on the erosional efficiency β_0. Grey line represents the change of RMS.

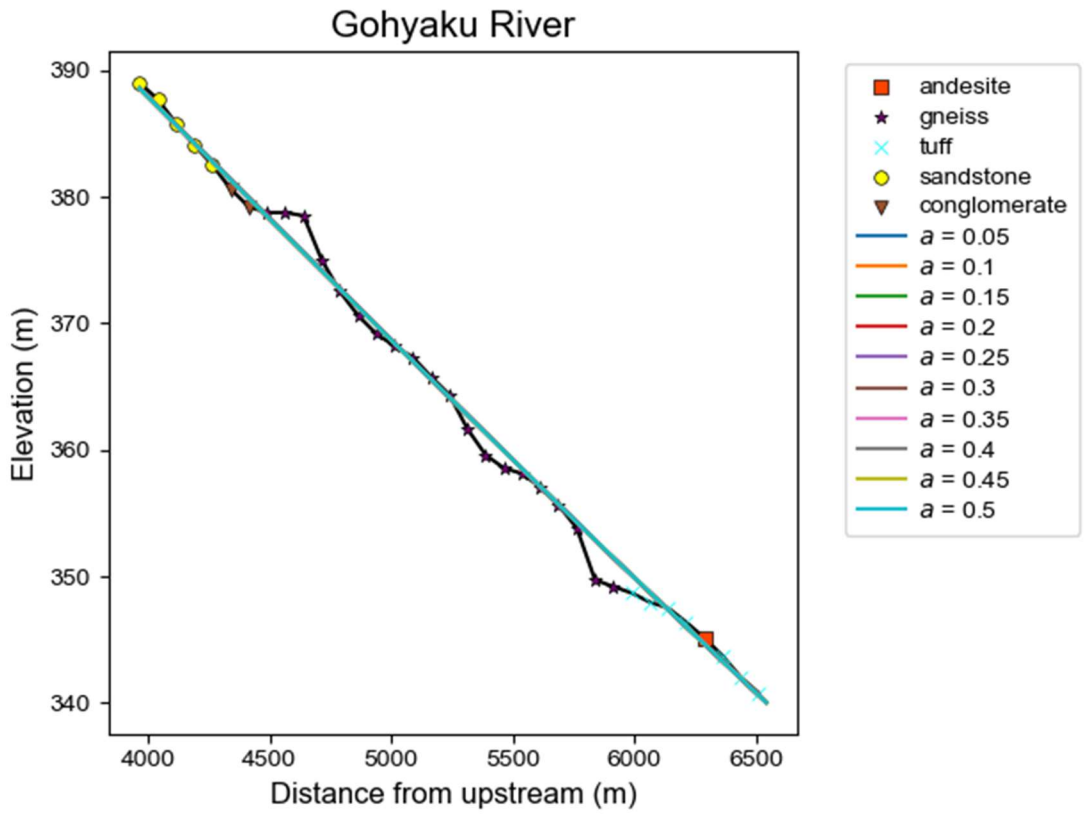

Figure S7. SFDM results of the Gohyaku River obtained by varying the value of bedload ratio *a*. Color dots indicate lithology along Gohyaku River (same as Fig.4), and the colored line represents the optimized model result. Within the tested range, changes in the ratio of the bedload to the total sediment supply do not significantly affect the optimized results.

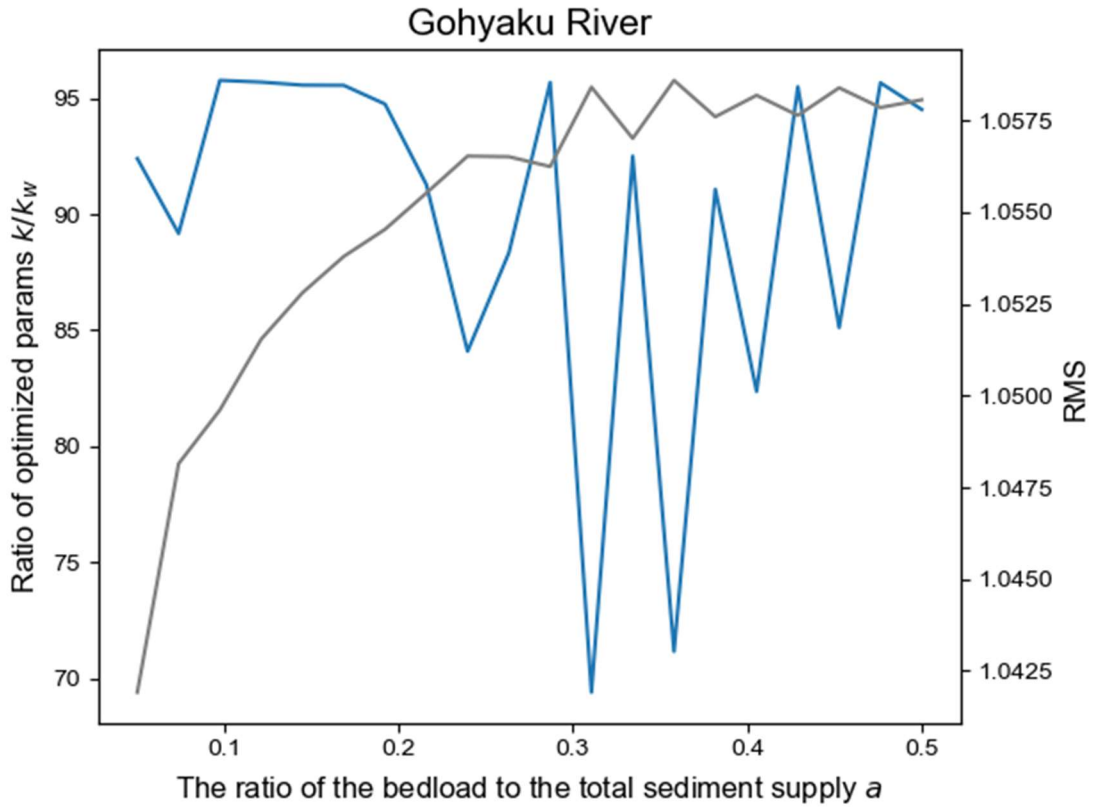

Figure S8. Relationship between ratio of the bedload to total sediment supply a, ratio of optimized parameters, and RMS. X-axis shows the ratio of the bedload to the total sediment supply a, and y-axis shows the ratio of optimized params k/k_w. Blue line represents the change of optimized params depending on the ratio of bedload to the total sediment supply a. Grey line represents the change of RMS. The ratio of optimized params k/k_w seems not to be related to the bedload ratio a.

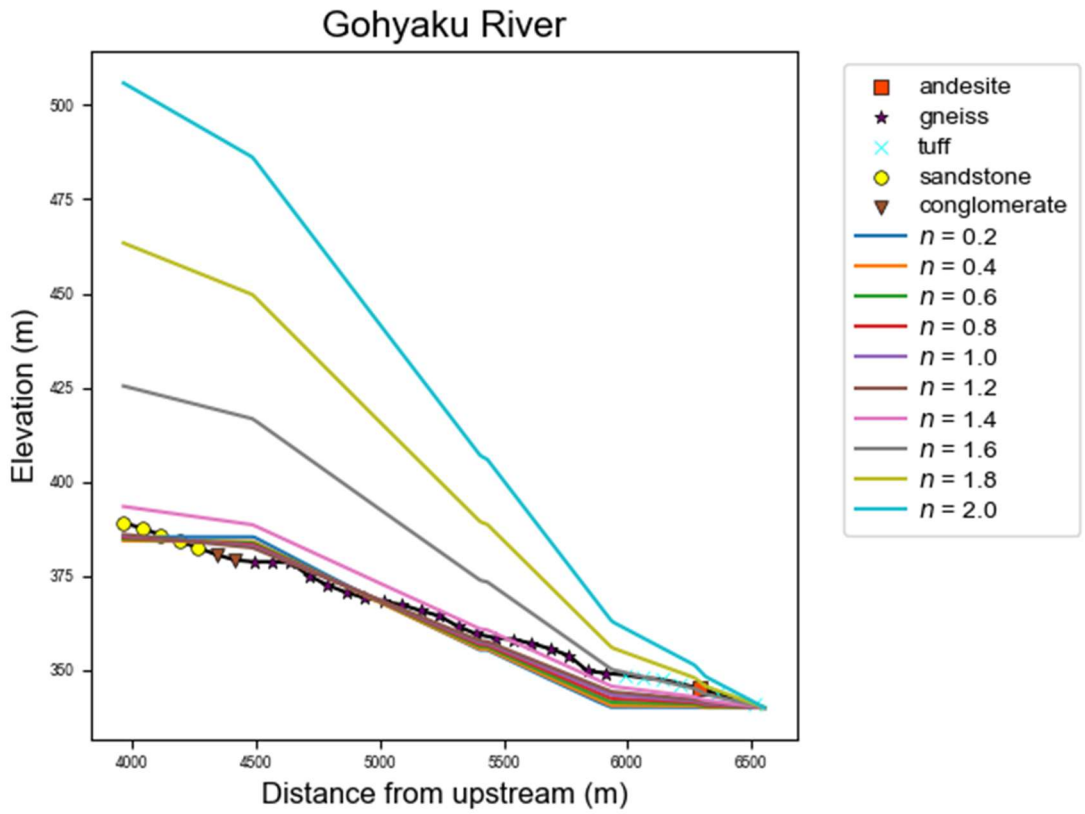

Figure S9. ASPM results of the Gohyaku River obtained by varying the slope exponent n.. Color dots indicate lithology along Gohyaku River (same as Fig.4), and the colored line represents the optimized model result. As n increases, the change in channel gradient at lithological boundaries becomes more gradual; however, when n exceeds ~1.5, gradients steeper than those of the present-day topography emerge, and the modeled profiles progressively diverge from the observed topography.

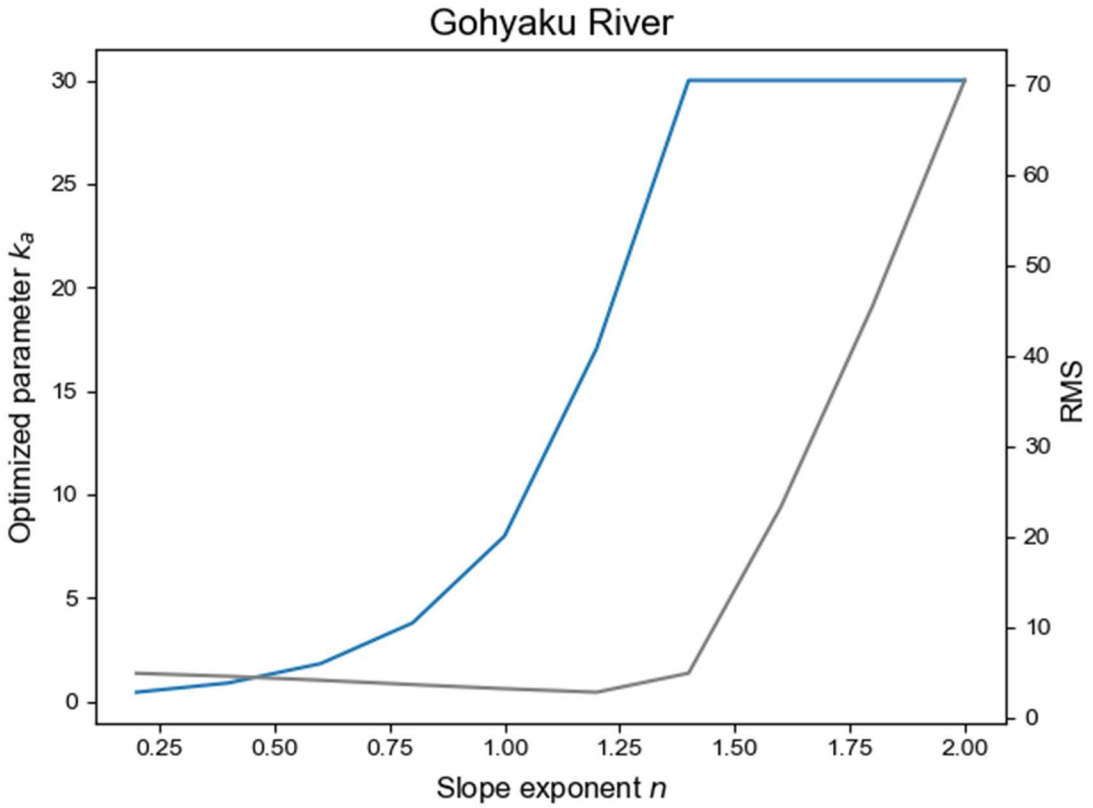

Figure S10. Relationship between slope exponent n, ratio of optimized params, and RMS in ASPM. X-axis shows the slope exponent n, and y-axis shows the value of optimized parameter k_a. Blue line represents the change of optimized params depending on slope exponent n. Grey line represents the change of RMS. Until slope exponent n becomes ~1.5, RMS is almost stable.

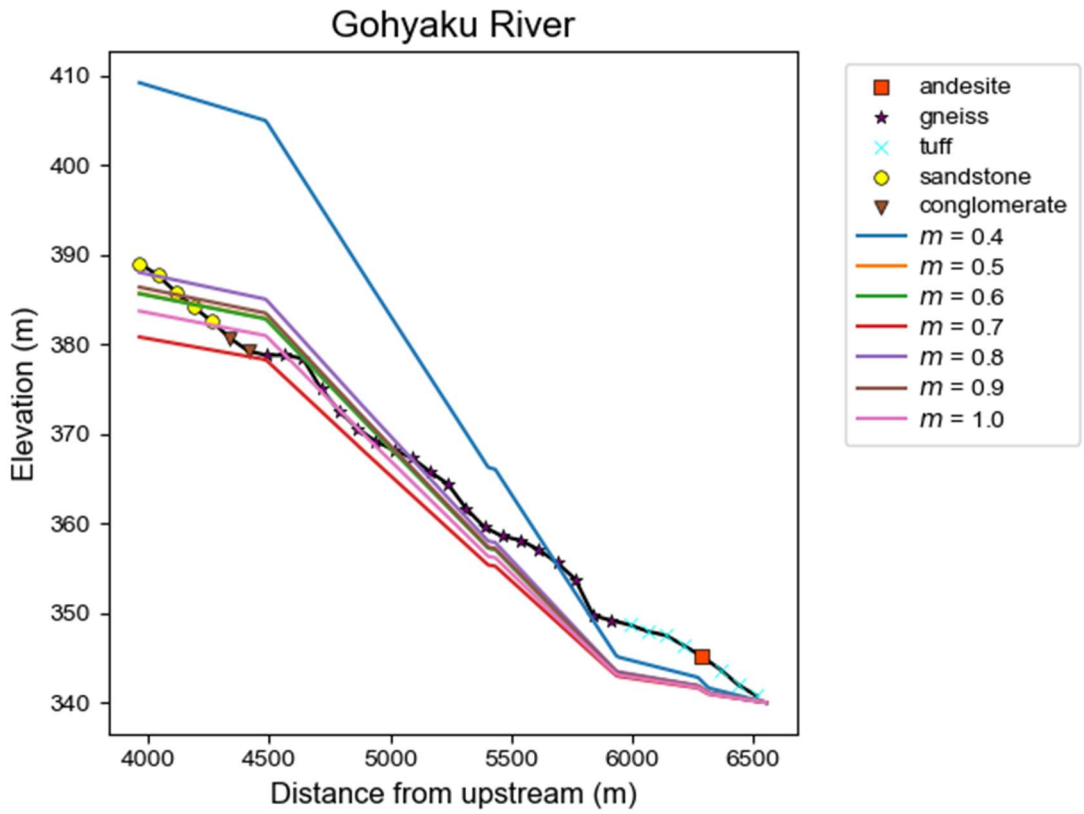

Figure S11. ASPM results of the Gohyaku River obtained by varying the drainage area exponent m. Color dots indicate lithology along Gohyaku River (same as Fig.4), and the colored line represents the optimized model result. As m increases, the change in channel gradient at lithological boundaries becomes more gradual.

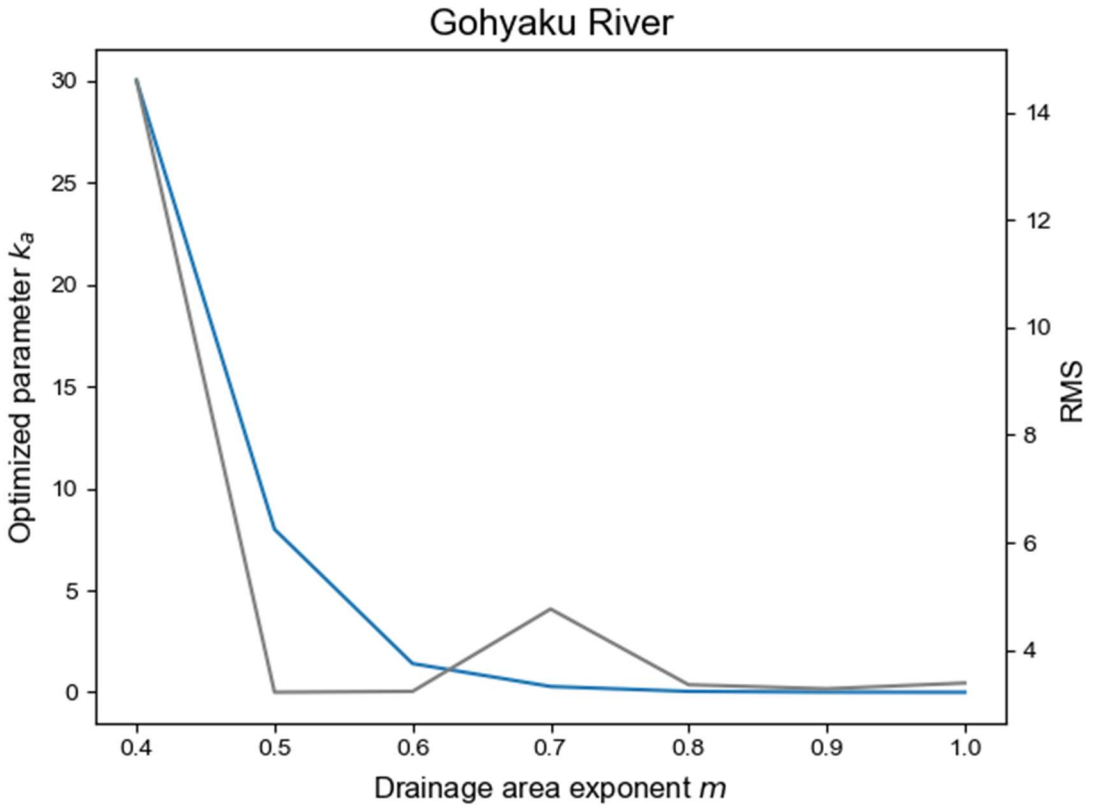

Figure S12. Relationship between drainage area exponent m, ratio of optimized params, and RMS in ASPM. X-axis shows drainage area exponent m, and y-axis shows the value of optimized parameter k_a. Blue line represents the change of optimized params depending on drainage area exponent m. Grey line represents the change of RMS. Over drainage area exponent $m = 0.5$, RMS is almost stable.

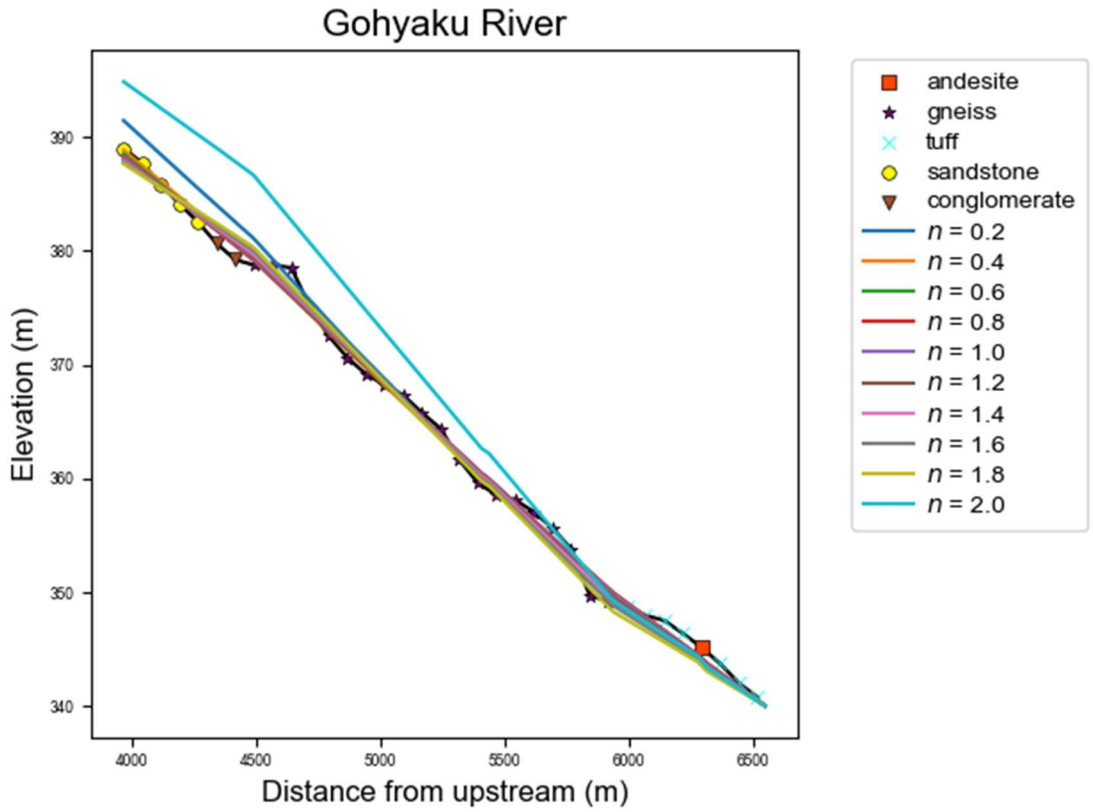

Figure S13. SPACEM results of the Gohyaku River obtained by varying the slope exponent n.. Color dots indicate lithology along Gohyaku River (same as Fig.4), and the colored line represents the optimized model result.

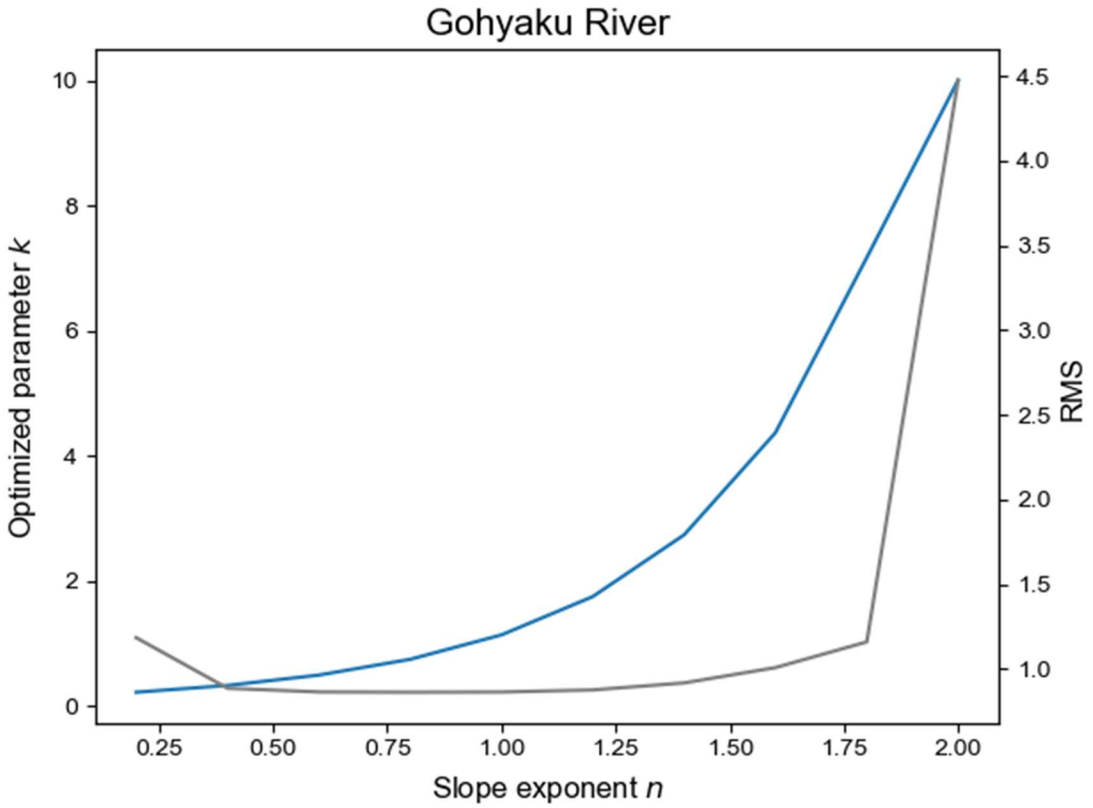

Figure S14. Relationship between slope exponent n, ratio of optimized params, and RMS in SPACEM. X-axis shows the slope exponent n, and y-axis shows the value of optimized parameters k. Blue line represents the change of optimized params depending on slope exponent n. Grey line represents the change of RMS. Until slope exponent n becomes ~1.8, RMS is almost stable.

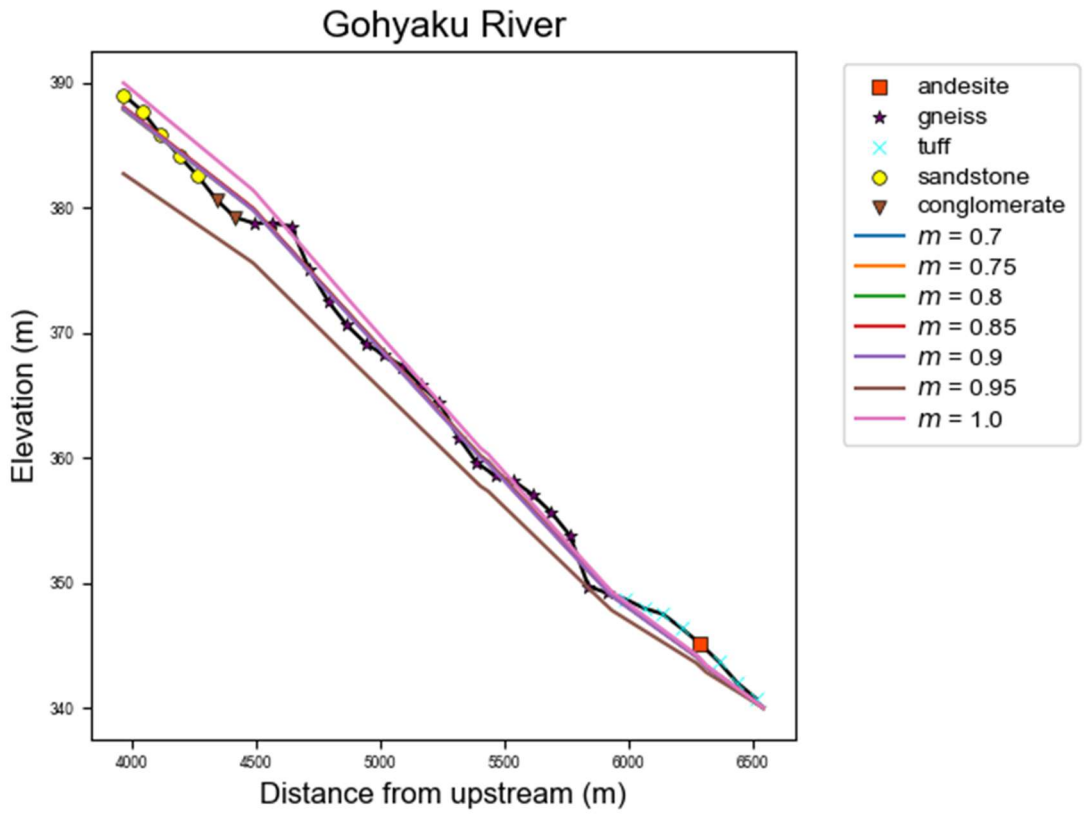

Figure S15. SPACEM results of the Gohyaku River obtained by varying the drainage area exponent m. Color dots indicate lithology along Gohyaku River (same as Fig.4), and the colored line represents the optimized model result.

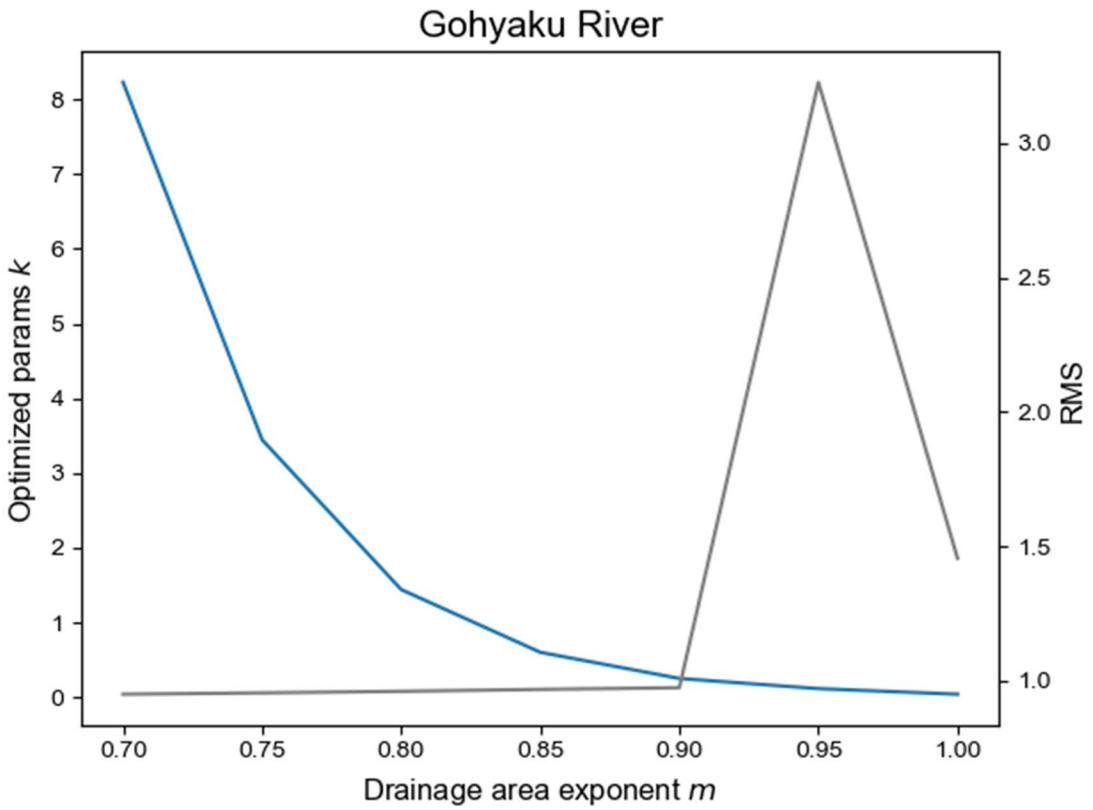

Figure S16. Relationship between drainage area exponent m, ratio of optimized params, and RMS in SPACEM. X-axis shows drainage area exponent m, and y-axis shows the value of optimized parameter k. Blue line represents the change of optimized params depending on drainage area exponent m. Grey line represents the change of RMS. Until drainage area exponent m becomes ~0.9, RMS is almost stable.

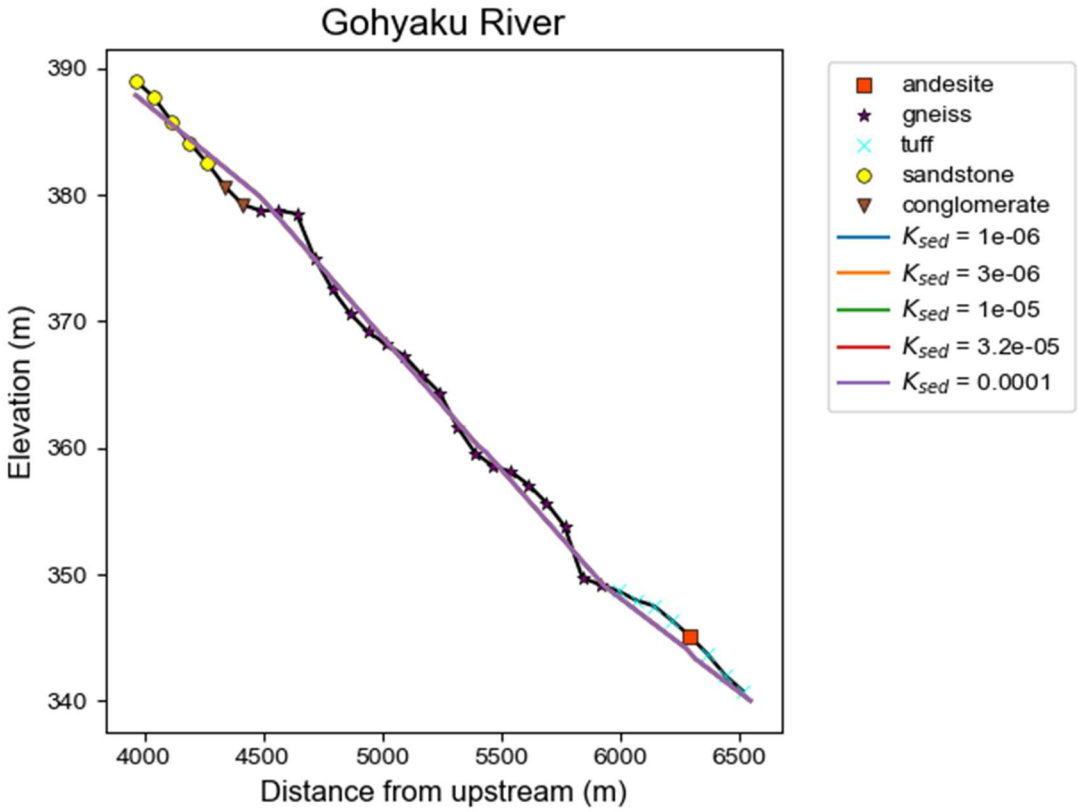

Figure S17. SPACEM results of the Gohyaku River obtained by varying sediment erodibility K_{sed}. Color dots indicate lithology along Gohyaku River (same as Fig.4), and the colored line represents the optimized model result. Calculated river profiles are indistinguishable.

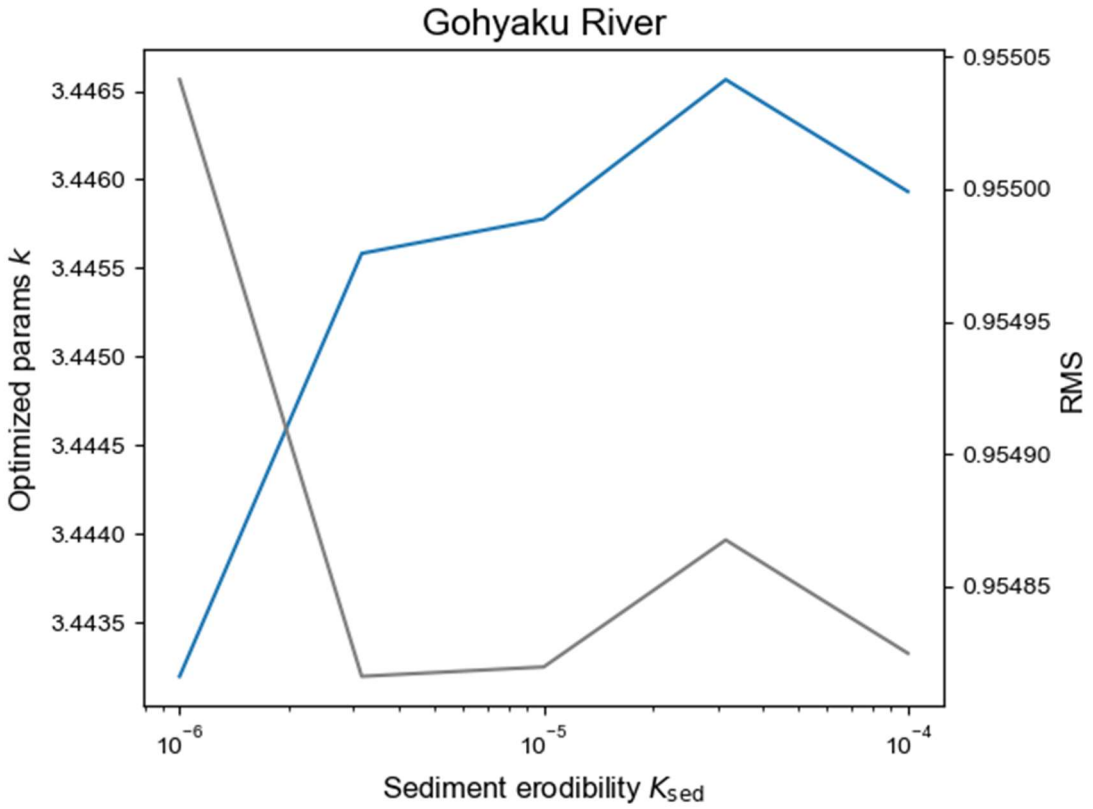

Figure S18. Relationship between sediment erodibility K_{sed}, ratio of optimized params, and RMS in SPACEM. X-axis shows the sediment erodibility K_{sed}, and y-axis shows the value of optimized parameter k. Blue line represents the change of optimized params depending on sediment erodibility K_{sed}. Grey line represents the change of RMS.

Reference SI

Akiba, T., Sano, S., Yanase, T., Ohta, T., and Koyama, M.: Optuna: A Next-generation Hyperparameter Optimization Framework, https://arxiv.org/abs/1907.10902, 2019.

Guryan, G. J., Johnson, J. P. L., and Gasparini, N. M.: Sediment Cover Modulates Landscape Erosion Patterns and Channel Steepness in Layered Rocks: Insights From the SPACE Model, Journal of Geophysical Research: Earth Surface, 129, e2023JF007 509,https://doi.org/https://doi.org/10.1029/2023JF007509, e2023JF007509 2023JF007509, 2024.

Inoue, T., Izumi, N., Shimizu, Y., and Parker, G.: Interaction among alluvial cover, bed roughness, and incision rate in purely bedrock and alluvial-bedrock channel, Journal of Geophysical Research: Earth Surface, 119, 2123–2146, https://doi.org/https://doi.org/10.1002/2014JF003133, 2014.

Takayama, S.: Study on Bedload Gravels in Mountain Streams near Kaifuura, Niigata Prefecture (Part II), Geological Review of Japan, 38, 415–425, https://doi.org/10.4157/grj.38.415, 1965.

Whipple, K. X. and Tucker, G. E.: Dynamics of the stream-power river incision model: Implications for height limits of mountain ranges, landscape response timescales, and research needs, Journal of Geophysical Research: Solid Earth, 104, 17 661–17 674, https://doi.org/https://doi.org/10.1029/1999JB900120, 1999.